Photon stimulated desorption processes including cracking of molecules in a vacuum chamber at cryogenic temperatures.

Article · January 1999

Source: OAI

CITATIONS
3

READS
163

4 authors, including:

Oleg Borisovich Malyshev
STFC Daresbury Laborarory Warrington
199 PUBLICATIONS **1,302** CITATIONS
SEE PROFILE

V. V. Anashin
Budker Institute of Nuclear Physics
139 PUBLICATIONS **978** CITATIONS
SEE PROFILE

Ian R Collins
Independent Researcher
61 PUBLICATIONS **1,020** CITATIONS
SEE PROFILE

EUROPEAN LABORATORY FOR PARTICLE PHYSICS

CERN - LHC DIVISION

LHC-VAC/OBM

Technical Note 99-13

October 1999

PHOTON STIMULATED DESORPTION PROCESSES INCLUDING CRACKING OF MOLECULES IN A VACUUM CHAMBER AT CRYOGENIC TEMPERATURES

O.B. Malyshev, V.V. Anashin, I. R. Collins and O. Gröbner

Abstract

The design of the LHC vacuum system requires a complete understanding of all processes which may affect the residual gas density inside the 1.9 K cold bore of the cryo-magnets. So far, a wealth of experimental data has been obtained which may be used to predict the residual gas density inside a cold vacuum system exposed to synchrotron radiation (SR). The purpose of this study has been to include for the first time in addition to the recycling, the effect of cracking of cryosorbed molecules by synchrotron radiation.

Cracking of molecular species like CO_2 and CH_4 have been observed in several recent studies and these findings have been incorporated in a more detailed dynamic gas density model for the LHC. In this note, we describe the relevant physical processes and the parameters required for a full evaluation.

It can be shown that the dominant gas species in the LHC vacuum system with its beam screen are H_2 and CO. The important result of this study is that while the surface coverage of cryosorbed CH_4 and CO_2 molecules is limited due to cracking, the coverage of H_2 and CO molecules may increase steadily during the long term operation of the LHC.

1 Introduction

Over most of its circumference, the LHC vacuum system consists of a cold bore tube inside the 1.9 K cryo-magnets, a perforated beam screen which is homed in the cold bore as to intercept beam induced effect such as synchrotron radiation (SR) and to carry image current. The experimental studies of photon stimulated desorption in a vacuum system with cryo-sorbing walls started in 1993 at the Budker Institute of Nuclear Physics (BINP, Novosibirsk, Russia) and at the Brookhaven National Laboratory (BNL, Upton, NY, USA) in the context of the SSC project. During these early studies it was found that the gas density in a cryogenic vacuum system consists, in the general case, of three parts: primary photodesorption of strongly bound chemisorbed molecules, secondary photodesorption of weakly bound cryosorbed molecules leading, in a closed system, to the repeated recycling of the same molecules, and finally thermal desorption corresponding to the vapour pressure given by the adsorption isotherm [1]. Subsequent studies found that some of the cryosorbed molecules, specifically CO_2 and CH_4, could be cracked to produce additional H_2, CO and O_2, which in turn must be taken also into account [2,3,4].

The main parameters necessary to predict the gas density in a cold beam tube were determined either on the beam lines of the VEPP-2M storage ring at BINP in collaboration with the SSCL [5,6,7] and with CERN [8,9,10] or at the EPA storage ring at CERN [4,11]. Recent studies, both at BINP [2,3] and at CERN [4], have highlighted the importance of the cracking of cryosorbed molecules by SR for the LHC. This effect had not been taken into account in earlier studies, and is addressed in this paper.

2 Photodesorption in a vacuum chamber with cryosorbing walls

The photodesorption processes in a vacuum chamber with cryosorbing walls has been studied extensively in the context of the SSC and the LHC projects [1,12,13].

In contrast to a conventional room temperature vacuum system, where the gas molecules are readily removed by external pumps, the gas molecules desorbed by the SR in a cryogenic system have a high probability to stick to the chamber wall after only a few wall interaction. External pumping from the ends is rather inefficient to remove the gas molecules and in fact it is appropriate to approximate a cryosorbing vacuum chamber as an infinitely long tube, thereby neglecting end pumping.

The more complete picture of the gas density in a cryosorbing vacuum system exposed to SR depends on the following processes:

1. The desorption of strongly bound chemisorbed molecules from the surface and near-surface layers of the vacuum chamber by SR, defined as primary desorption.
2. The desorption of weakly bound physisorbed molecules by SR. These molecules may represent a substantial surface coverage due to the non-zero sticking probability on the cryosorbing wall. The photodesorption yield of these cryosorbed molecules is defined as the secondary photodesorption, in contrast to the primary desorption, or alternatively the recycling coefficient, illustrating the fact that molecules present in the system are repeatedly redesorbed and recondensed on the walls. This recycling effect clearly depends on surface density of cryosorbed molecules [1].
3. The thermal equilibrium between surface and volume gas densities, i.e. the vapour pressure corresponding to the specific adsorption isotherm, for sufficiently large coverages must also be included. This contribution to the gas density depends on the surface characteristics, the surface coverage and the temperature [1,5,14]. Finally, also the sticking probability of molecules depends on the its surface coverage, on the characteristics of the surface and on temperature [2].
4. The additional process, which has been included in this study, is the transformation through cracking of condensed gas molecules from one species to one or more other species. For instance, CO_2 molecules have been observed to produce CO and O_2. Due to this effect, the

amount of condensed CO_2 can be reduced while, at the same time, it constitutes an additional source of CO and O_2 molecules [2–4].

Incorporating these physical processes into an existing model to describe the photo-stimulated desorption for a cryogenic vacuum system [12], the balance for each individual gas species can be written as:

$$V\frac{dn_i}{dt} = h_i\dot{\Gamma} + h_i'(s_i)\dot{\Gamma} + c_i(s_j)\dot{\Gamma} - a_i S_i\left(n_i - n_{e_i}(s_i)\right) - C_i n_i; \quad (1)$$

$$A\frac{ds_i}{dt} = a_i S_i\left(n_i - n_{e_i}(s_i)\right) - h_i'(s_i)\dot{\Gamma} - k_{i\to k+m}(s_i)\dot{\Gamma}; \quad (2)$$

where the index i denotes the gas species in the residual gas spectrum;

n *[molecules/cm^3]* is the volume molecular density;

s *[molecules/cm^2]* is the surface molecular density;

V *[cm^3]* is the vacuum chamber volume;

A *[cm^2]* is the vacuum chamber wall area;

$\dot{\Gamma}$ *[photon/sec]* is the photon intensity;

h *[molecules/photon]* is the primary photodesorption yield;

h' *[molecules/photon]* is the secondary photodesorption yield;

a is the sticking probability;

$S_i = A\bar{v}_i / 4$ *[cm^3/sec]* is the ideal wall pumping speed, $\bar{v}_i$ is mean molecular speed for the gas i;

C *[cm^3/sec]* is the distributed pumping speed provided by the slots in the LHC beam screen;

n_e *[molecules/cm^3]* is the thermal equilibrium gas density.

Finally,

$k_{i\to k+m}(s_i)$ *[molecules/photon]* is the cracking efficiency of type i molecules into type k and type m (i.e. how well the type i molecules could be cracked per photon);

$c_i(s_j)$ *[molecules/photon]* is the cracking yield of the type i molecules from the type j molecules, (i.e. how many the type i molecules are created due to cracking of the type j molecules per photon). This parameter is a secondary parameter of cracking efficiency of gases, which produces type i molecules due to cracking.

In other words, k expresses the removal of one molecular species due to cracking into molecules of other species and c expresses the production of a molecular species through cracking of some other, parent, molecule. The value of c are derived from k :

$$c_i(s_j) = a_{i,j} k_{j \to i+n}(s_j),$$

the coefficient $a_{i,j}$ is a ratio between the number of molecules type i produced by cracking to the number of cracked molecules type j.

It can be seen that the gas density of a vacuum system at cryogenic temperatures depends on a number of parameters which, to a large extent, are not well known and thus will need to be determined experimentally. The limited amounts of available experimental results have been compiled in Section 3. The important input parameters include not only the temperature T but also the critical photon energy ε_c of the SR and the accumulated photon dose, Γ. It should be noted that several of the variables appearing in the model depend implicitly on the surface coverage.

The equations (1) and (2) may be simplified for two special cases which are particularly relevant for the design of the LHC vacuum system: a bare cold bore tube, i.e. a cold bore without a beam screen, and a system which incorporates a beam screen with pumping holes. These two cases are characterised by the condition C = 0 and C > 0 respectively.

2.1 LHC cold bore without a beam screen

The gas density inside a long cold bore can be obtained by neglecting the gas flow towards both ends of the system. This approach approximates a 'closed system' which is independent of any boundary conditions and gives a uniform longitudinal density distribution. In addition, since in the practical analysis one is generally not interested in the fast transient behaviour but rather in the slow density evolution over many hours of photon irradiation, the following 'quasi-static' approximations can be made:

$$V \frac{dn_i}{dt} \approx 0 \text{ and } A \frac{ds_i}{dt} \neq 0$$

Under these simplifying assumptions, the quasi-static gas density of each species is given by:

$$n_i = \frac{\left(h_i + h'_i(s_i) + c_i(s_j)\right)\dot{\Gamma}}{a_i S_i} + n_e(s_i) \ . \qquad (3)$$

It should be noted that under otherwise constant conditions there exists an implicit dependence of the recycling coefficient h¢, the sticking probability a, the cracking yield c, as well as the thermal vapour pressure n_e on the surface coverage. Furthermore, the cracking term c, which depends on the coverage of the parent-type molecules, leads to an effective coupling of the different cryosorbed species by transforming one type into molecules of another type.

The time dependant surface density *s(t)* of the cryosorbed molecules may be computed through the integral:

$$s_i(t) = s_i(0) + \frac{1}{A}\int_{t=0}^{t}\left(h_i(t) + c_i(s_j(t)) - k_i(s_i(t))\right)\dot{\Gamma}\,dt \ . \qquad (4)$$

where the parameters in the integral depend on the time varying surface coverage of each individual molecular species. The third term depends on the surface density s_j of the cryosorbed molecules of the type j which could be cracked with appearance molecules of the type *i*.

It is interesting to obtain an estimate of the maximum gas density which can occur in the system by assuming that all three parameters, the secondary desorption yield and both of the cracking yields increase with the surface coverage up to a maximum value h_{max}, k_{max} and c_{max} respectively. Under this condition the density would have the upper bound:

$$n_i \le \frac{\left(h_i + h'_{i\max} + \sum_{j\neq i} c_{i\max}(s_j)\right)\dot{\Gamma}}{a_i S_i} + n_{e_i} \ . \qquad (5)$$

A more restricting estimation can be made for vacuum chamber, which had no precondensed gas before the irradiation gets started. In this case only the gas which is desorbed during irradiation can be cracked, i.e. $h_j \ge k_{j\to i+k} = a_{i,j}\,c_i(s_j)$, hence:

$$n_i \le \frac{\left(h_i + h'_{i\max} + \sum_{j\neq i} \frac{h_j}{a_{i,j}}\right)\dot{\Gamma}}{a_i S_i} + n_{e_i} \ . \qquad (6)$$

where h_j is the photodesorption yield of gases which could produce the gas *i* due to cracking.

A simpler estimation can be made for the gases which can be cracked by photons, $k_{i\to j+k}(s_i) \neq 0$, but which could not appear due to the cracking of other species, $c_i(s_m) = 0$.

$$n_i \leq \frac{(h_i + h'_{i\max})\dot{\Gamma}}{a_i S_i} + n_{e_i}. \qquad (7)$$

For these gases, when the initially bare surface irradiated by photons, $k_i(s_i)$ will increase until it reaches its maximal value $k_{i\max}(s_i) = h_i$ because the number of molecules, which can be cracked, can not be greater than the number of desorbed molecules. In this case a new condition occurs in the vacuum chamber: $A\frac{ds_i}{dt} \approx 0$. Let us define a new parameter r_i, which is a ratio of saturated values of secondary desorption yield and cracking efficiency: $r_i = h'_{i\max}(s_i)/k_{i\max}(s_i)$, then $h'_i < h'_{i\max} = r_i k_{i\max} = r_i h_i$. So the gas density can be estimated as:

$$n_i \leq \frac{h_i \dot{\Gamma}(1 + r_i)}{a_i S_i} + n_e(s_i). \qquad (8)$$

2.2 LHC cold bore with a beam screen

The analysis of a cold bore system with beam screen and pumping holes proceeds in an similar manner to the previous section. The configuration with distributed pumping holes is characterised by C > 0, hence by a non-vanishing linear pumping speed in addition to the wall pumping. Furthermore, following the argument in the previous section, the same approximation of slowly varying gas density and surface coverage can be made by assuming

$$V\frac{dn}{dt} \approx 0 \text{ and } A\frac{ds}{dt} \neq 0.$$

The quasi-static gas density in the system is given by:

$$n_i = \frac{\left(h_i \dot{\Gamma} + h'_i(s_i) + c_i(s_j)\right)\dot{\Gamma} + s_i S_i n_e(s_i)}{a_i S_i + C_i}. \qquad (9)$$

Contrary to the solution with a bare cold bore, the surface density s on the beam screen is effectively limited by the distributed pumping C of the holes in the screen and is given by the expression:

$$s_i(t) = s_i(0) + \frac{1}{A}\int_{t=0}^{t}\left[\left(h_i(t) + c_i(s_j(t)) - k_i(s_i(t))\right)\dot{\Gamma} - C_i n_i(t)\right]dt \ . \qquad (10)$$

Under conditions where the thermal equilibrium density n_e can be neglected, the slowly varying gas density inside the beam screen can be written in an alternative form:

$$n_i(t) = \frac{\left(h_i(t) + c_i(s_j(t)) - k_i(s_i(t))\right)\dot{\Gamma}}{C_i} - \frac{A}{C_i}\frac{ds_i}{dt}. \qquad (11)$$

Ultimately, when the surface coverage has reached a constant value, i.e. $A\frac{ds}{dt} \approx 0$, the gas density becomes constant and independent of the wall pumping speed:

$$n_i = \frac{(h_i + c_i(s_j) - k_i(s_i))\,\dot{\Gamma}}{C_i}. \qquad (12)$$

Furthermore, in the equilibrium state

$$h_j \geq k_{j\rightarrow i+k} = a_{i,j}\,c_i(s_j),$$

hence, there is an upper limit for the gas i density

$$n_i \leq \frac{\left(h_i + \sum_{j\neq i}\frac{h_j}{a_{i,j}}\right)\dot{\Gamma}}{C_i}, \qquad (13)$$

where h_j is the photodesorption yield of gases which could produce the gas i due to cracking.

For the gases which can be cracked by photons, $k_{i\rightarrow j+k}(s_i) \neq 0$, but which can not appear due to the cracking of other species, $c_i(s_m) = 0$, the limitation of the gas density depends only on primary desorption and distributed pumping speed:

$$n_i \le \frac{h_i \dot{\Gamma}}{C_i}, \qquad (14)$$

3 Experimentally determined parameters.

3.1 Primary desorption yields for H_2, CH_4, CO and CO_2

The primary photodesorption coefficient, h, as a function of accumulated number of photons with a critical energy of e_c = 50 eV [8] shown in Figure 1 can be modelled by:

$$h = h_0 \, (\Gamma_0/\Gamma)^{0.33}, \qquad (15)$$

where h_0 is the photodesorption yield corresponding to the accumulated number of photons, Γ_0.

These experimental data were obtained from experiments with the LHC beam screen prototype at T = 78 K irradiated by photons with a critical energy of about 50 eV.

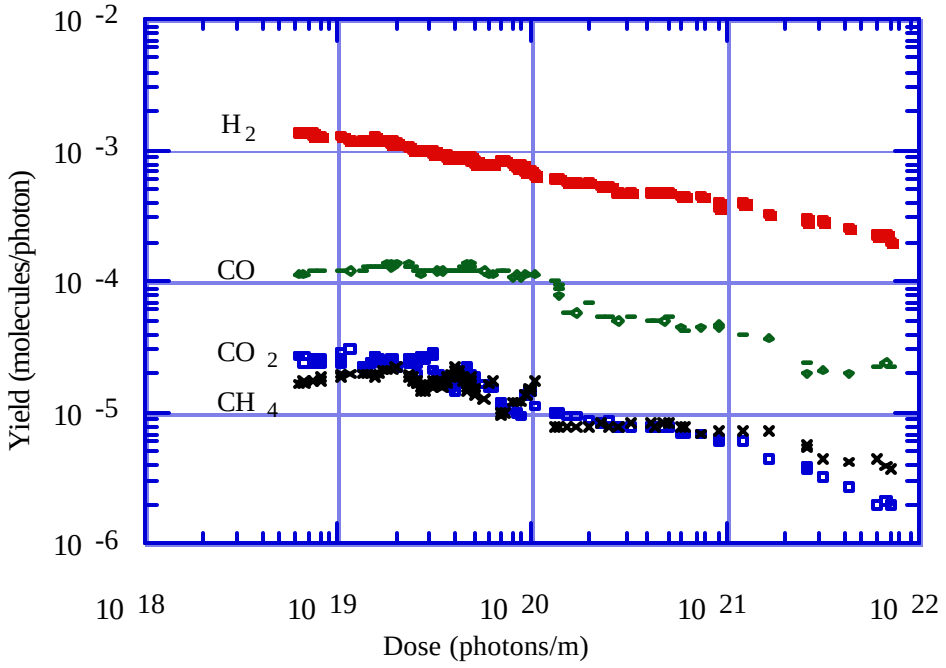

Figure 1. Primary photodesorption yield as function of accumulated photon dose at T=78 K [8].

Experimental photodesorption data exist for photon doses between 10^{19} to 10^{22} photons/m [1,5,6,8]; the photodesorption yields at higher accumulated photon doses are estimated with Equation (15). Table 1 shows the experimental data [8] and extrapolated data for the accumulated photon doses in the range 10^{19} to 10^{24} photons/m which will be used in the following estimations. The accumulated photon doses may be converted to the operating time of the LHC assuming nominal beam current and neglecting any reducing, commissioning of the LHC. For nominal photon intensity $\dot{\Gamma} = 10^{17}$ photon/(sec·m), one hour of the LHC operating time corresponds to the accumulated photon dose of $3.6 \cdot 10^{20}$ photons/m. The row "Operating time" in Table 1 shows the time of LHC operating at nominal current for the arcs, i.e. with the photon flux of 10^{17} photon/(sec·m).

Table 1. Photodesorption yield for different gases at cryogenic temperatures

Γ, [photons/m]	10^{19}	10^{20}	10^{21}	10^{22}	10^{23}	10^{24}
Operating time	106 sec	18 min	3 hrs.	30 hrs.	12 days	4 months
Photodesorption yield, [molecules/photon]						
Gases	Experimental data				Estimated values	
H_2	$2 \cdot 10^{-3}$	$8 \cdot 10^{-4}$	$4 \cdot 10^{-4}$	$2 \cdot 10^{-4}$	$9 \cdot 10^{-5}$	$5 \cdot 10^{-5}$
CH_4	$2 \cdot 10^{-5}$	$1 \cdot 10^{-5}$	$7 \cdot 10^{-6}$	$3 \cdot 10^{-6}$	$1.5 \cdot 10^{-6}$	$9 \cdot 10^{-7}$
CO	$2 \cdot 10^{-4}$	$1 \cdot 10^{-4}$	$5 \cdot 10^{-5}$	$2 \cdot 10^{-5}$	$1 \cdot 10^{-5}$	$5 \cdot 10^{-6}$
CO_2	$3 \cdot 10^{-5}$	$1 \cdot 10^{-5}$	$7 \cdot 10^{-6}$	$2 \cdot 10^{-6}$	$1 \cdot 10^{-6}$	$5 \cdot 10^{-7}$
Total amount of desorbed molecules/m						
H_2	$2 \cdot 10^{16}$	$1.0 \cdot 10^{17}$	$6.0 \cdot 10^{17}$	$3 \cdot 10^{18}$	$1.8 \cdot 10^{19}$	$9 \cdot 10^{19}$
CH_4	$2 \cdot 10^{14}$	$1.1 \cdot 10^{15}$	$7.5 \cdot 10^{15}$	$4.5 \cdot 10^{16}$	$3 \cdot 10^{17}$	$1.3 \cdot 10^{18}$
CO	$2 \cdot 10^{15}$	$1.1 \cdot 10^{16}$	$6.9 \cdot 10^{16}$	$3 \cdot 10^{17}$	$2 \cdot 10^{18}$	$9 \cdot 10^{18}$
CO_2	$3 \cdot 10^{14}$	$1.2 \cdot 10^{15}$	$7.5 \cdot 10^{15}$	$4 \cdot 10^{16}$	$2 \cdot 10^{17}$	$9 \cdot 10^{17}$

These data can be compared with the data for hydrogen from the same paper for a beam screen at 5 K to 10 K [8]. At the lower temperature the initial photodesorption yield for H_2 is 5 times lower, but the

cleaning effect due to photons is also reduced, i.e. the photodesorption yields are the same at the dose of 10^{22} photons/m. The signal for other gases was below the RGA sensitivity in that experiment.

The data in Table 1 can be also compared with data in ref. [11]. The ratio of photodesorption yields for different gases at LHe and LN_2 temperatures was specially studied by V. Baglin [4]. There it was shown that the ratio of initial photodesorption yields of different gases changes with temperature. In particular, the ratio $h(CO) / h(CO_2) \approx 1$ at T = 4.2 K was obtained. A very "pessimistic" estimation with the consequence that the data for CO_2 increased by an even larger factor of 50 is made in this paper especially for this case.

3.2 Secondary desorption yield and cracking of molecules

The gas molecules condensed on the cryogenic surface can be removed from the surface by SR in two ways: either as a whole molecule (so-called secondary desorption or desorption of cryosorbed molecules) or as cracked species of these molecules [2–4].

In the experiments performed in the 'closed geometry', the measured value was the gas pressure which can be converted into $(h+h¢)/a$ or $(h+h¢+c)/a$ in the case of cracking, i.e. it is only possible extract from this experiment the ratio $h¢/a$ and c/a. In the 'closed geometry' experiments the ratio $h¢/a$ for H_2 was measured. This value increases with increasing surface coverage and reaches a saturation value of about 5 molecules/photon at the surface coverage of about $3 \cdot 10^{15}$ molecules/cm^2 [1]. The same value was measured for the surface coverage of 10–20 times higher [2]. For other gases (CH_4, CO and CO_2), only the upper limit of this value was measured [9]:

$$(h+h¢)/a \approx 10^{-3} \text{ molecules/photon.}$$

The experiments performed in the 'open geometry' the photodesorption yield of cryosorbed molecules is not affected by the sticking probability a [2,3,10]. The removal efficiency, h_r', i.e. how many molecules condensed on the cold substrate can be removed from the substrate per photon, was measured for all cryosorbed gases H_2, CH_4, CO and CO_2 and was found to increase with increasing surface coverage and to reach a saturation value.

This saturation value is about 0.55 molecules/photon for H_2 at $3 \cdot 10^{15}$ molecules/cm^2.

For CH_4, CO and CO_2, the saturation values reached at the surface coverage of three orders of magnitude higher (~10^{19} molecules/cm^2) and the are 0.45, 0.4 and 0.04 molecules/photon for CO_2, CH_4 and CO respectively.

The removal efficiency, h_r', was obtained from amount of cryosorbed gas before irradiation, Q_1, amount of desorbed gas after irradiation, Q_2 and photon dose, Γ: $h_r' = (Q_1 - Q_2)/\Gamma$. This includes molecules removed from the substrate by two effects: secondary desorption and cracking: $h_r' = h' + k$. The ratio h'/k can be estimated from the gas spectrum analysis. It was concluded from results of experiments [2,3,10]:

- The desorption processes of cryosorbed CO_2 and CH_4 molecules involves mostly cracking of these molecules:

$$h_r'(CO_2) = h'(CO_2) + k_{CO_2 \to CO+O} \quad \text{and} \quad h_r'(CH_4) = h'(CH_4) + k_{CH_4 \to 2H_2+C}.$$

- The cracking efficiency is about 10 times higher than the secondary desorption for both of these gases [2–4]:

$$r_{CO_2} = \frac{h'(CO_2)}{k_{CO_2 \to CO+O}} \approx \frac{1}{10} \quad \text{and} \quad r_{CH_4} = \frac{h'(CH_4)}{k_{CH_4 \to 2H_2+C}} \approx \frac{1}{10}.$$

- No dependency of the observed desorption-removal process on temperature in the range 5.5K to 20K for CH_4, 5.5K to 15K for CO and 5.5K to 68K for CO_2 was found [2,3].

The parameter of the cracking yield c is a secondary parameter of the cracking efficiency k. For example, the CO_2 cracking process gives one molecule of CO and one atom of O, hence, $c_{CO}(s_{CO_2}) = k_{CO_2 \to CO+O}$ and $c_{O_2}(s_{CO_2}) = 0.5 k_{CO_2 \to CO+O}$.

The CH_4 cracking process gives two molecules of H_2 and one atom of C, hence, $c_{H_2}(s_{CH_4}) = 2k_{CH_4 \to 2H_2+C}$ and $c_C(s_{CH_4}) = k_{CH_4 \to 2H_2+C}$. For an estimation of the upper limit of the gas density, it is necessary to take into account the possibility of process: $CH_4 + CO_2 + \tilde{g} \to 2H_2 + 2CO$, in this case: $c_{CO}(s_{CO_2} + s_{CH_4}) = k_{CO_2 \to CO+O} + k_{CH_4 \to 2H_2+C}$.

Maximal values of the parameters describing the secordary desorption and the cracking are presented in Table 2.

Table 2. Maximal values of secondary desorption and cracking parameters.

	H_2	CH_4	CO	O_2	CO_2
$h'_{r\max}$	0.55	0.4	0.04	—	0.45
$h'_{\max}$	0.55	0.04	0.04	no data	0.04
$k_{\max}$	—	$k_{CH_4\to 2H_2+C} \approx$ ≈ 0.36	—	—	$k_{CO_2\to CO+O} \approx$ ≈ 0.41
$c_{\max}$	$c_{H_2}(s_{CH_4}) \approx$ ≈ 0.72	—	$c_{CO}(s_{CO_2}+s_{CH_4}) \approx$ $\approx 0.41+0.36$	$c_{O_2}(s_{CO_2}) \approx$ ≈ 0.2	—

There are no experimental data on photodesorption of cryosorbed O_2, so it is assumed in our estimation to have the same value as for CO, i.e. $h'_{\max}(O_2) = 0.04$.

3.3 Sticking probability

The value of the sticking probability can be in the range of $0 \le \alpha \le 1$ and depends on the nature of gas, the temperature of both the gas and the surface, the surface material, the surface conditions (clean or not, roughness) and etc.

The sticking probability α for H_2 could be estimated from experiments with a beam screen [6,15] :

$\alpha \approx 0.1$ with ε_c = 284 eV and T_{bs} = 4.2K;

$\alpha \approx 0.5$ with ε_c = 50 eV and T_{bs} = 5–11 K.

The sticking probability α for CO is expected to be close to 1.

Meanwhile there are some experimental data for the sticking probability of CO_2 [2] and H_2 [16], which indicate that the sticking probability could be close to zero on a surface without precondensed gas and increase to about unity with a surface coverage.

3.4 Thermal equilibrium gas density

Many researchers studied the gas density inside a vacuum chamber at cryogenic temperaturesas function of temperature, surface nature and molecular coverage [17], molecular flux [18], time of gas deposition [9], presence of other gases (gas mixtures) [14]. The gas density depends of each of these parameters. It is more difficult to estimate the gas density at low surface coverage (less than one monolayer) when sticking probability is undefined.

In general, one can conclude that is impossible to predict the thermal gas density in a real vacuum chamber with many parameters changing with time. To avoid this problem the gas density is studied at extremely low or high coverage, i.e. when the thermal gas density is either much less than both the dynamic gas density due to photodesorption and the lifetime limit or much higher than the lifetime limit. The saturated thermal gas density is negligible for all gases at 1.9 K. At 4.5 K the saturation gas density for H_2 is about 10^{13} molecules/cm^3, which is much higher than the lifetime limit for the LHC (10^9 molecules/cm^3).

3.5 The mean molecular speed

A mean molecular speed of $v \approx 8 \cdot 10^4$ cm/s corresponding to a gas temperature of about 60 K has been measured at a critical photon energy of e_c = 284 eV for photodesorbed H_2 molecules [7]. There are no experimental data for other molecules or for e_c = 44 eV. One may assume that the mean molecular speed for desorbed H_2 at e_c = 44 eV could be less than for e_c = 284 eV.

For H_2 this factor could be:

$$k_{e_c} = \frac{\bar{v}(e_c = 44.1eV)}{\bar{v}(e_c = 284eV)} = \sqrt{\frac{44.1}{248}} = 0.4$$

This will increase our estimations by a factor of 2.5 for H_2.

For all other gases, the mean molecular speeds have not been measured, but one may assume that the velocity should scale with the ratio of the molecular mass M_{gas}:

$$k_M = \sqrt{\frac{M_{H_2}}{M_{gas}}}\,.$$

For CO $k_M = 0.27$ and for CO_2 $k_M = 0.21$, resulting in an increase in the gas density by factor of 9.5 and 12 for CO and CO_2, respectively.

In other words, this assumption gives the mean speed of photodesorbed molecules, which corresponds to about 10 K, i.e. in the range of the beam screen operating temperature (between 5 K and 20 K). Since the lowest gas temperature gives a more 'pessimistic' estimation (i.e. higher gas density), the reduced mean molecular speed is used.

4 Estimation of upper limit for the dynamic gas density inside the LHC vacuum chamber

There are four main photodesorbed gases in a cryogenic vacuum chamber: H_2, CH_4, CO and CO_2, and two of them (CH_4 and CO_2) can be cracked by photons, $\tilde{g}$:

$$CH_4 + \tilde{g} \rightarrow C + 2H_2 \quad \text{and} \quad 2CO_2 + \tilde{g} \rightarrow 2CO + O_2 . \qquad (16)$$

The addition amount of H_2, CO and O_2 appears in a vacuum chamber due to photo-cracking of CH_4 and CO_2. Since $h_{CO_2} >> h_{CH_4}$, we will assume here that there are no free radicals:

$$k_1 CH_4 + k_2 CO_2 + \tilde{g} \rightarrow 2k_1 H_2 + (k_1 + k_2) CO + \left(\frac{k_2}{2} - k_1 \right) O_2 . \qquad (17)$$

As it was shown in Section 2, one can estimate the upper limit of gas density in a vacuum chamber. In this section these estimations are done the LHC vacuum chambers.

4.1 LHC cold bore without a beam screen

The upper limit of the gas density for H_2, CO and O_2 can be estimated from equation (5) in the following way. The maximal value of both the secondary desorption yield and the cracking yield are much higher than the primary desorption yield for H_2, CO and O_2. The saturated value of the equilibrium gas density, $n_{e\max}$, are negligible at T= 1.9 K and T= 4.5 K all gases except H_2 at T= 4.5 K. Hence, the upper limit of the gas density for H_2 and CO could be estimated, in case when surface coverage is unknown, as:

$$n_{H_2} \le n_{e\max}, \text{ at } T = 4.5K \quad (18)$$

$$n_{H_2} \le \frac{\left(h'_{H_2\max} + c_{H_2\max}(s_{CH_4})\right)\dot{\Gamma}}{a_{H_2} S_{H_2}}, \text{ at } T = 1.9K \quad (19)$$

$$n_{CO} \le \frac{\left(h'_{CO\max} + c_{CO\max}(s_{CO_2}) + c_{CO\max}(s_{CH_4})\right)\dot{\Gamma}}{a_{CO} S_{CO}}, \quad (20)$$

$$n_{O_2} \le \frac{\left(h'_{O_2\max} + c_{O_2\max}(s_{CO_2})\right)\dot{\Gamma}}{a_{O_2} S_{O_2}}. \quad (21)$$

For a vacuum chamber with walls with some amount of precondensed gas the equation (6) should be used, then we have:

$$n_{H_2} \le n_{e\max}, \text{ at } T = 4.5K \quad (22)$$

$$n_{H_2} \le \frac{h'_{H_2\max}\dot{\Gamma}}{a_{H_2} S_{H_2}}, \text{ at } T = 1.9K \quad (23)$$

$$n_{CO} \le \frac{\left(h'_{CO\max} + h_{CO_2} + h_{CH_4}\right)\dot{\Gamma}}{a_{CO} S_{CO}}, \quad (24)$$

$$n_{O_2} \le \frac{\left(h'_{O_2\max} + 0.5h_{CO_2}\right)\dot{\Gamma}}{a_{O_2} S_{O_2}}. \quad (25)$$

Cryosorbed CH_4 and CO can be cracked with SR. Following equation (7) for an unknown initial surface coverage the maximal gas densities are

$$n_{CH_4} \le \frac{h'_{CH_4\max}\dot{\Gamma}}{a_{CH_4} S_{CH_4}}, \quad (26)$$

$$n_{CO_2} \le \frac{h'_{CO_2\max}\dot{\Gamma}}{a_{CO_2} S_{CO_2}}. \quad (27)$$

For the vacuum chamber with walls without precondensed gas the equation (8) should be used:

$$n_{CH_4} \le \frac{h_{CH_4}(1+r_{CH_4})\dot{\Gamma}}{a_{CH_4} S_{CH_4}}, \quad (28)$$

$$n_{CO_2} \le \frac{h_{CO_2}(1+r_{CO_2})\dot{\Gamma}}{a_{CO_2} S_{CO_2}}. \quad (29)$$

4.2 LHC cold bore with a beam screen

The upper limit of the gas density for H_2 and CO can be estimated for the equilibrium state as:

$$n_{H_2} \le \frac{(h_{H_2} + 2h_{CH_4})\dot{\Gamma}}{C_{H_2}}, \quad (30)$$

$$n_{CO} \le \frac{(h_{CO} + h_{CO_2} + h_{CH_4})\dot{\Gamma}}{C_{CO}}, \quad (31)$$

$$n_{O_2} \le \frac{0.5 h_{CO_2}\dot{\Gamma}}{C_{O_2}}. \quad (32)$$

Hence the gas density for CH_4 and CO_2 could be estimated as:

$$n_{CH_4} \le \min\left\{\frac{h_{CH_4}\dot{\Gamma}}{C_{CH_4}}, \frac{h_{CH_4}(1+r_{CH_4})\dot{\Gamma}}{s_{CH_4} S_{CH_4}}\right\}, \quad (33)$$

$$n_{CO_2} \le \min\left\{\frac{h_{CO_2}\dot{\Gamma}}{C_{CO_2}}, \frac{h_{CO_2}(1+r_{CO_2})\dot{\Gamma}}{s_{CO_2} S_{CO_2}}\right\}. \quad (34)$$

The numerical results of the upper limit estimation for the LHC are presented in Table 3.

Table 3. Upper limits gas density in the LHC vacuum chamber.

	$n(H_2)$, $[H_2/cm^3]$	$n(CH_4)$, $[CH_4/cm^3]$	$n(CO)$, $[CO/cm^3]$	$n(O_2)$, $[O_2/cm^3]$	$n(CO_2)$, $[CO_2/cm^3]$
Vacuum chamber without a beam screen (any surface coverage)					
T = 1.9 K	$5.1 \cdot 10^{10}$	$2.3 \cdot 10^{9}$	$6.1 \cdot 10^{10}$	$1.9 \cdot 10^{10}$	$3.7 \cdot 10^{9}$
T = 4.5 K	$n_e \approx 10^{13}$	$1.5 \cdot 10^{9}$	$3.9 \cdot 10^{10}$	$1.2 \cdot 10^{10}$	$2.4 \cdot 10^{9}$
Vacuum chamber without a beam screen (without precondensed gas)					
T = 1.9 K	$2.2 \cdot 10^{10}$	$1.2 \cdot 10^{6}$	$3.0 \cdot 10^{9}$	$3.2 \cdot 10^{9}$	$3.1 \cdot 10^{6}$
T = 4.5 K	$n_e \approx 10^{13}$	$8.1 \cdot 10^{5}$	$1.9 \cdot 10^{9}$	$2.1 \cdot 10^{9}$	$2.0 \cdot 10^{6}$
Vacuum chamber with a beam screen					
T = 5 K	$8.2 \cdot 10^{8}$	$2.3 \cdot 10^{7}$	$3.6 \cdot 10^{8}$	$2.4 \cdot 10^{7}$	$5.6 \cdot 10^{7}$
T = 20 K	$4.1 \cdot 10^{8}$	$1.2 \cdot 10^{7}$	$1.8 \cdot 10^{8}$	$1.2 \cdot 10^{7}$	$2.8 \cdot 10^{7}$

5 Dynamic gas density inside the LHC vacuum chamber

The calculations were made for the gas density inside the LHC vacuum chamber with and without a beam screen using the 'pessimistic' input value for the primary photodesorption yield shown in Table 1 and Figure 1 for the photon intensity as in the arcs, i.e. 10^{17} photons/(sec·m). As it was mentioned in Section 2, only the solutions for the infinitely long vacuum chambers are considered. The pumping at the end of vacuum chamber could improve the vacuum if the vacuum chamber is short [13]. Hence, the gas density estimations for either a long vacuum chamber or the upper limit of gas density for the any length vacuum chamber are made.

It should be noted that if the gas density will be increase beyond the lifetime limit of the LHC then the machine would require warming-up to desorb the condensed gases.

5.1 The gas density inside a vacuum chamber without a beam screen.

The estimation of gas density (equation (**3**)), the surface coverage (equation (**4**)) and the secondary desorption yields as function of accumulated photon dose are presented in Figure 2. The main gas in the vacuum chamber is H_2, although CO is second gas in spectrum, it is much less than H_2.

The dynamic processes in vacuum chamber are quite sensitive to effect of cracking. The gas density and the surface coverage (and, hence, the secondary desorption) of CH_4 and CO_2 are limited due to the cracking. Figure 3 demonstrates the estimation with the same parameters but without taking into account the effect of cracking. Here there is no limitation of the gas density, the surface coverage and the secondary desorption yield for CH_4 and CO_2. In that case the main gas in the vacuum chamber is H_2, and its density is the same. Although the gas density of CH_4, CO and CO_2 are comparable they is much less then H_2.

5.2 The gas density inside a vacuum chamber with a beam screen.

The LHC beam screen will be held at temperature in the range of 5 to 20 K. The gas density is shown for two extreme conditions for T = 20 K in Figure 4 and for T = 5 K in Figure 5. The surface coverage, *s*, and the secondary photodesorption yield, h', are also shown.

Figure 4 demonstrates that at relatively high temperatures (T = 20 K), the H_2 gas density reaches its maximum value almost instantly (for $a = 0.01$ and lower). At lower temperatures (see Figure 5), there is some finite pumping capacity of the cold walls of the beam screen ($a = 0.5$) and the initial gas density is less than the maximum value which is reached after about 15–20 minutes (corresponding to 10^{20} photons/m) of LHC operating conditions. There is no difference in the shape of the curves at higher accumulated photon doses. However, due to the different molecular speed, there is a difference in the absolute value with a factor $\sqrt{T_1/T_2} = \sqrt{20K/5K} = 2$, i.e. the gas density is two times lower at T = 20 K than at 5 K for all gases. At both temperatures, the H_2 gas density is limited by pumping through the holes of the beam screen.

The shape of the gas density curves for CH_4 and CO_2 is very similar to the one for H_2, but for a different reason. The surface coverage of these gases is limited by cracking and consequently, the

secondary desorption yields of these molecules are limited and comparable with the primary desorption yield.

The initial shape of the curve for CO gas density also looks the same until an accumulated photon dose of 10^{22} photons/m is reached (about one day of LHC operation), from then onwards, the CO gas density reaches its lowest value and then raises slowly due to the secondary desorption. This CO gas density does not reach the saturated value limited by pumping holes even after an accumulated photon dose of 10^{24} photons/m (about four months of LHC operation).

Figure 6 demonstrates the estimation with the same parameters but without taking in account the effect of cracking.

In Figure 2 to Figure 5, the primary desorption of CO is much higher than that for the gases which can be cracked: i.e. $h(CO) >> h(CO_2)$, $h(CO) >> h(CH_4)$. In some studies $h(CO_2)$ is higher than one used in this paper, as it was discussed in Section 3.1. Hence it is interesting to study how the results change when $h(CO_2) >> h(CO)$. In the calculations presented in Figure 7 a value $h(CO_2)$ was increased by a factor of 50 compared with the previous estimations; all other parameters remained as before. The CO_2 gas density is 50 times higher in Figure 7 due to the larger primary photodesorption, while the shape of this curve remains the same. However the shape of the CO gas density becomes slightly different. An additional peak appears in the range between 10^{21} and 10^{23} photons/m due to the significant cracking of CO_2 molecules. Hence, we may conclude that for the doses below $(2–3)\cdot10^{20}$ photons/m, the CO gas density depends only on the primary desorption. With the increasing dose, the main source of CO becomes photocracking of cryosorbed CO_2. Starting from the dose of about $3\cdot10^{22}$ photons/m, the secondary desorption becomes significant and from then onwards is the dominant process in photodesorption of CO. The main gas species in this case are H_2 and CO_2 until a dose about 310^{22} photons/m (about 2–3 days of the LHC operation), after that the main gas species in this case are H_2 and CO.

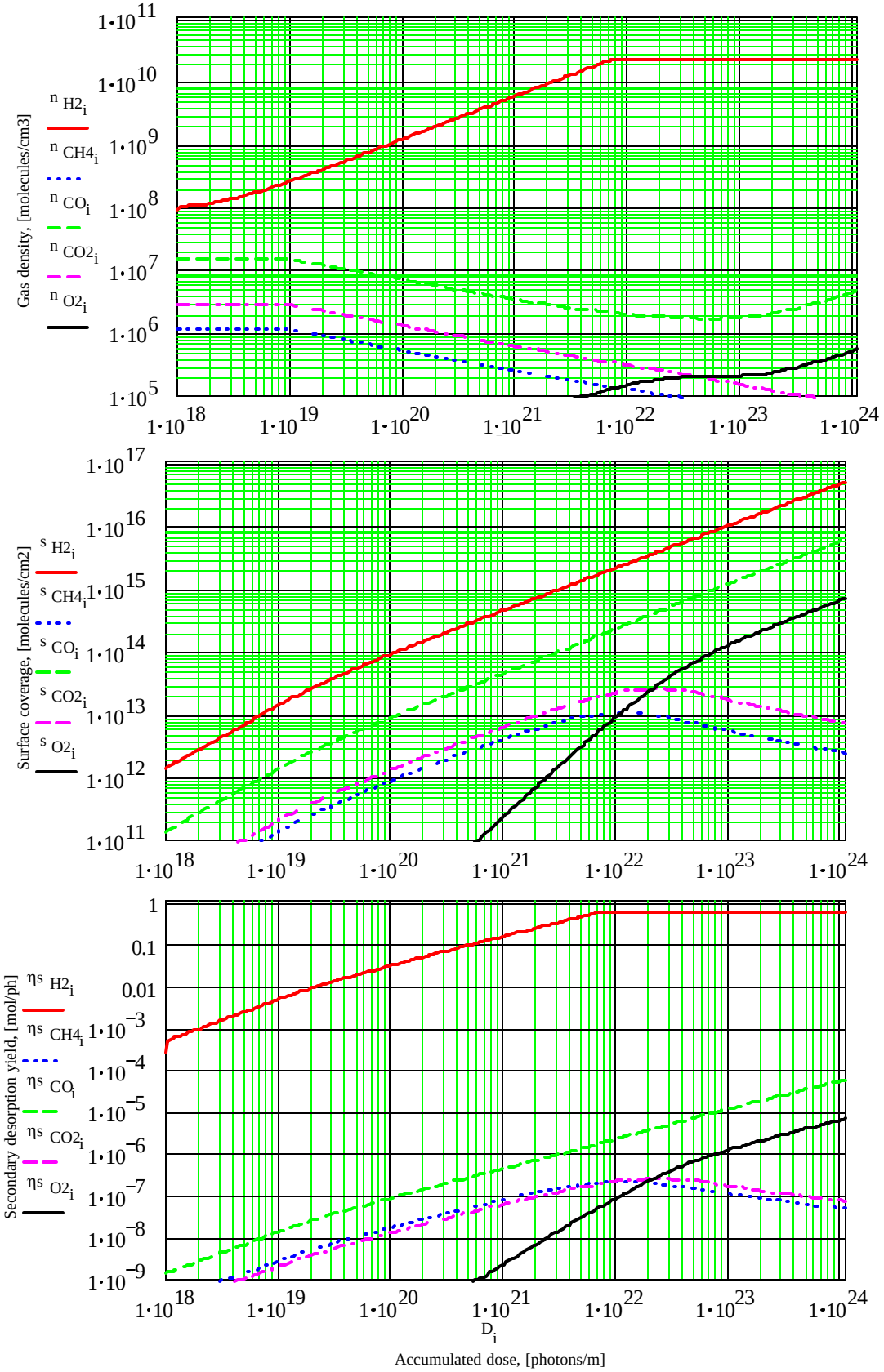

Figure 2. The gas density *n*, the surface coverage *s* and the secondary photodesorption yield η' in a vacuum chamber at T=1.9K without a beam screen.

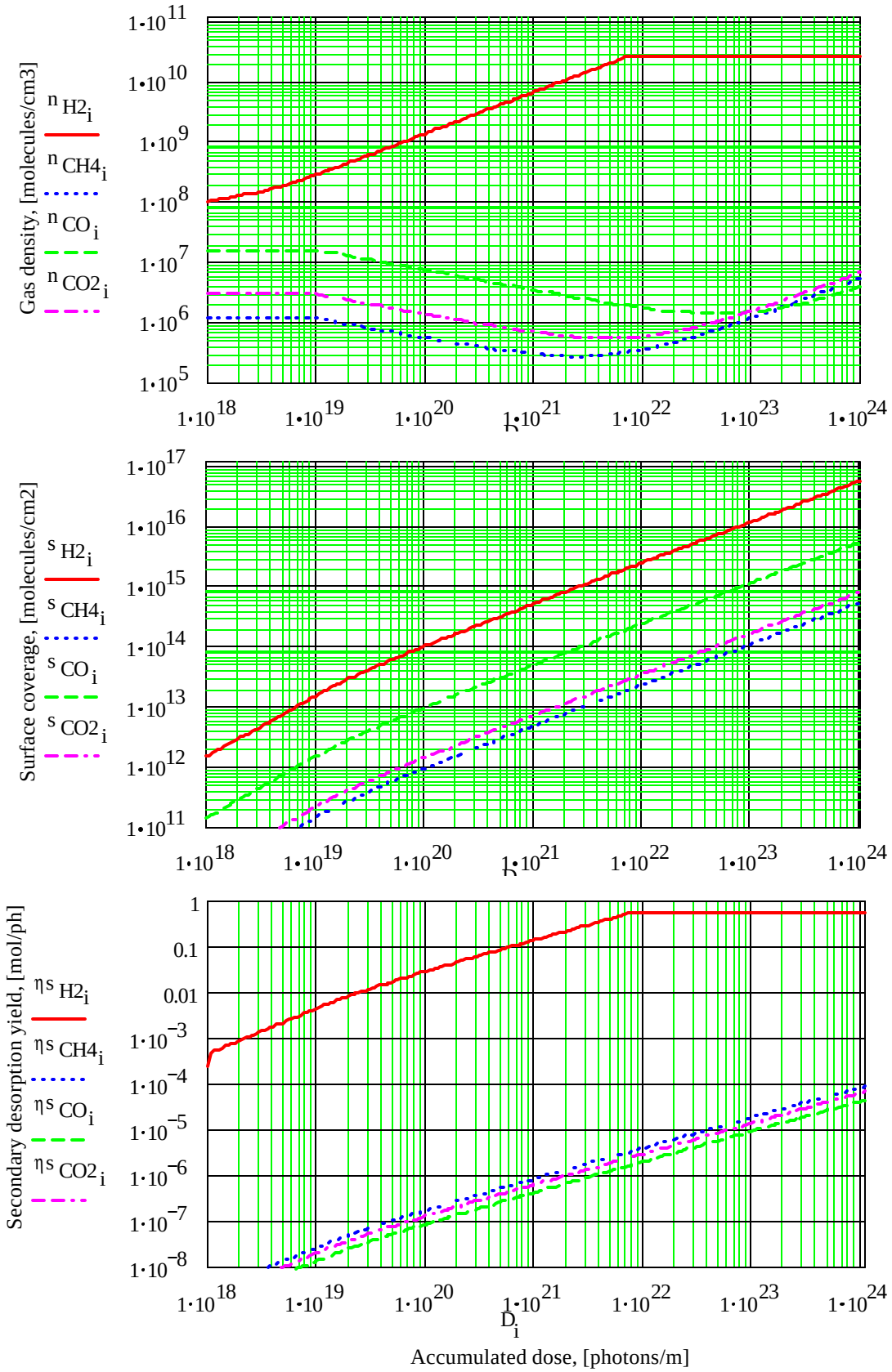

Figure 3. The gas density *n*, the surface coverage *s* and the secondary photodesorption yield η' in a vacuum chamber at T=1.9K without a beam screen *without taking in account the effect of cracking*.

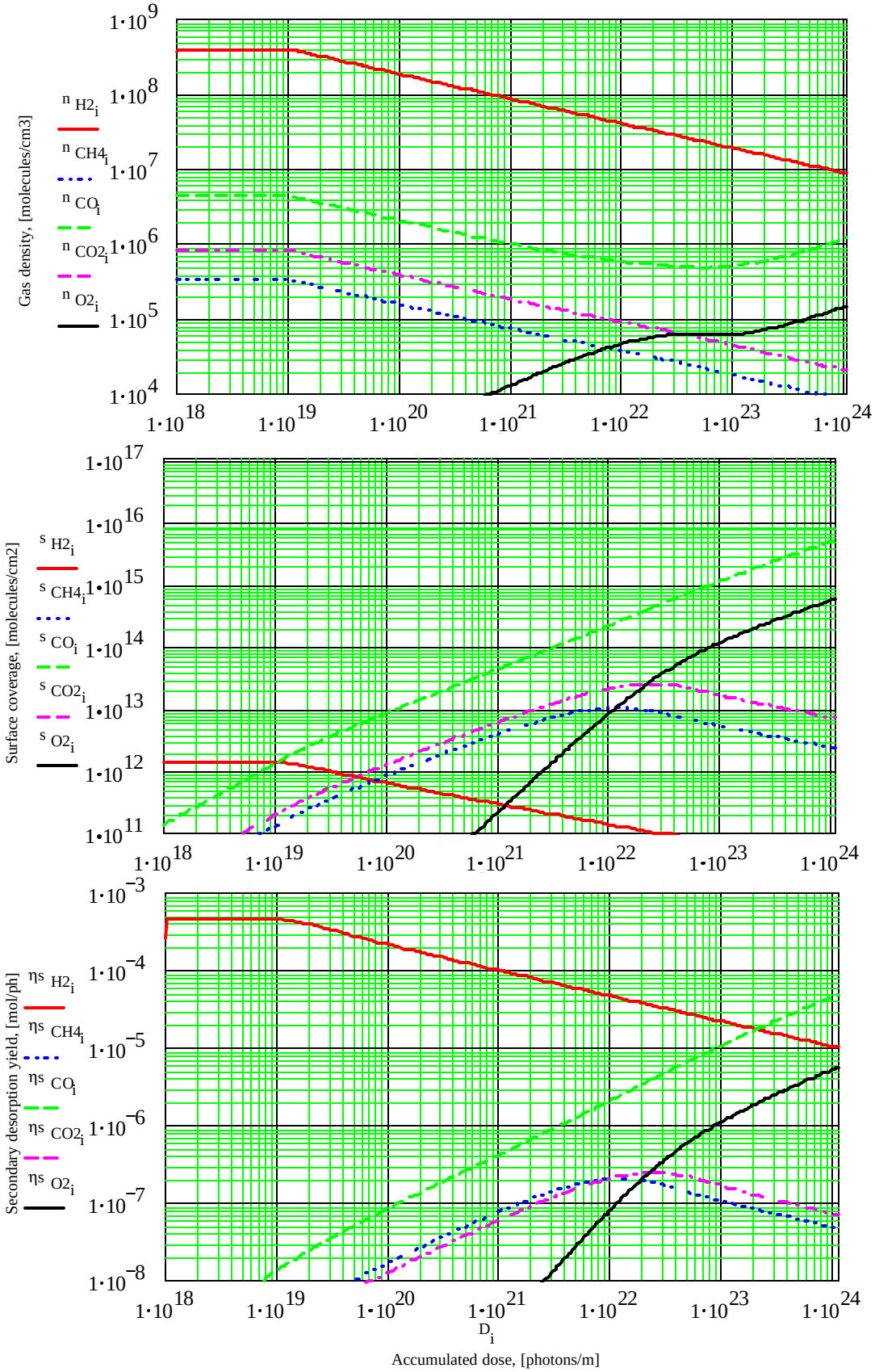

Figure 4. The gas density *n*, the surface coverage *s* and the secondary photodesorption yield η' in a vacuum chamber with a beam screen at T=20K ($a(H_2)$=0.01, $a(CH_4,CO,O_2,CO_2)$=1).

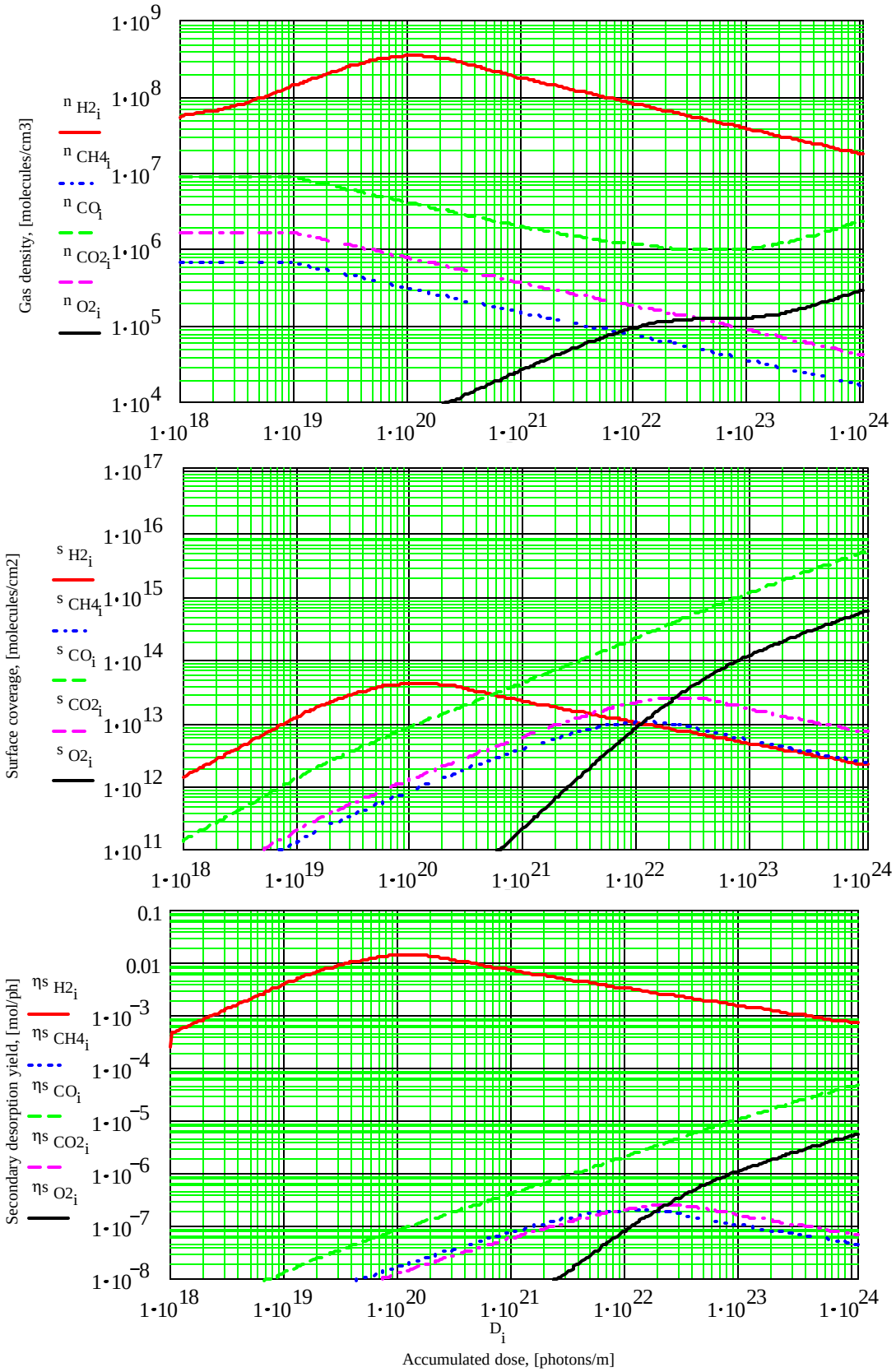

Figure 5. The gas density *n*, the surface coverage *s* and the secondary photodesorption yield η' in a vacuum chamber with a beam screen at T=5K ($a(H_2)$=0.5, $a(CH_4,CO,O_2,CO_2)$=1).

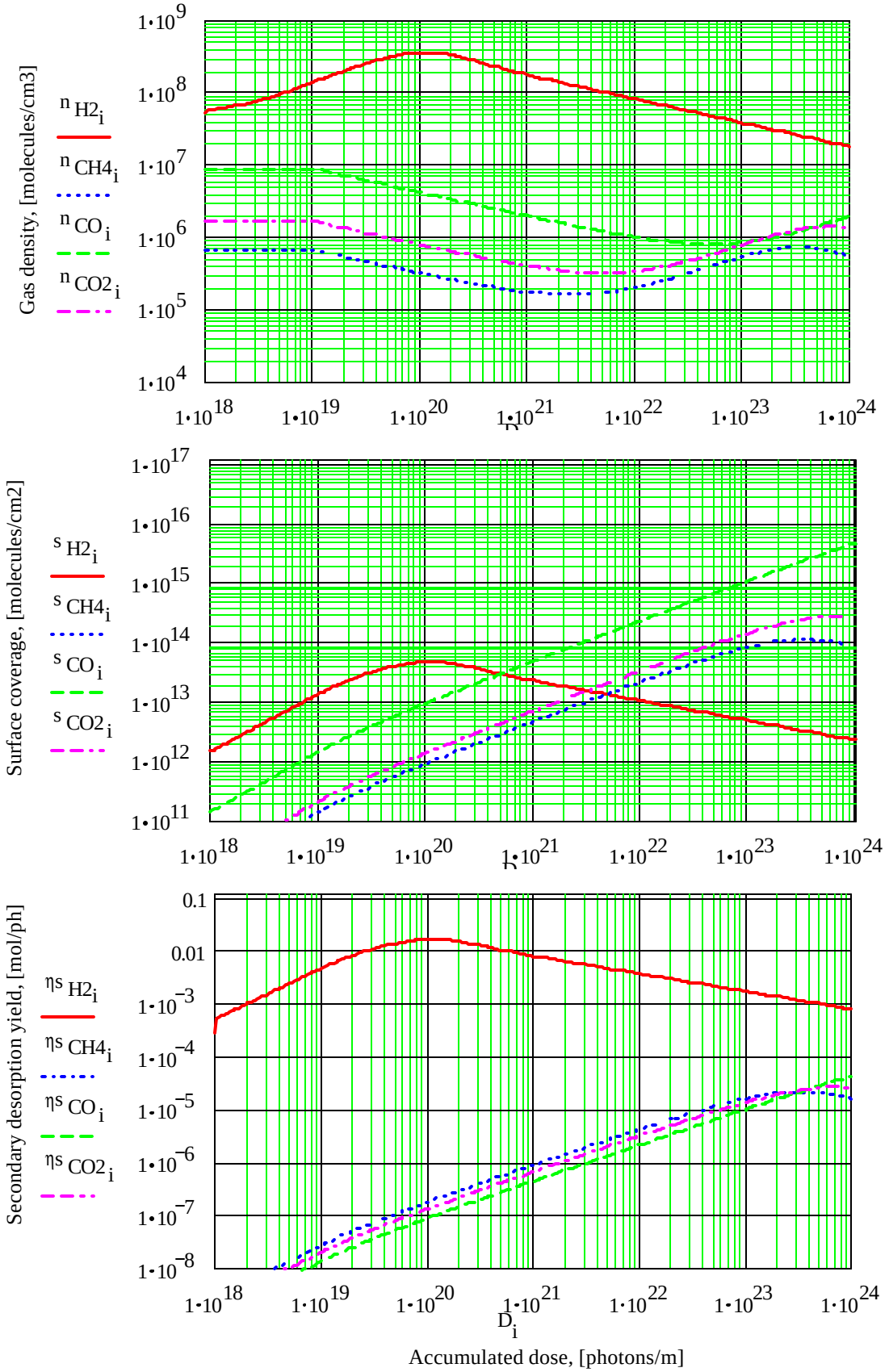

Figure 6. The gas density *n*, the surface coverage *s* and the secondary photodesorption yield η' in a vacuum chamber with a beam screen at T=5K ($\alpha(H_2)$=0.5, $\alpha(CH_4,CO,CO_2)$=1) *without taking in account the effect of cracking*.

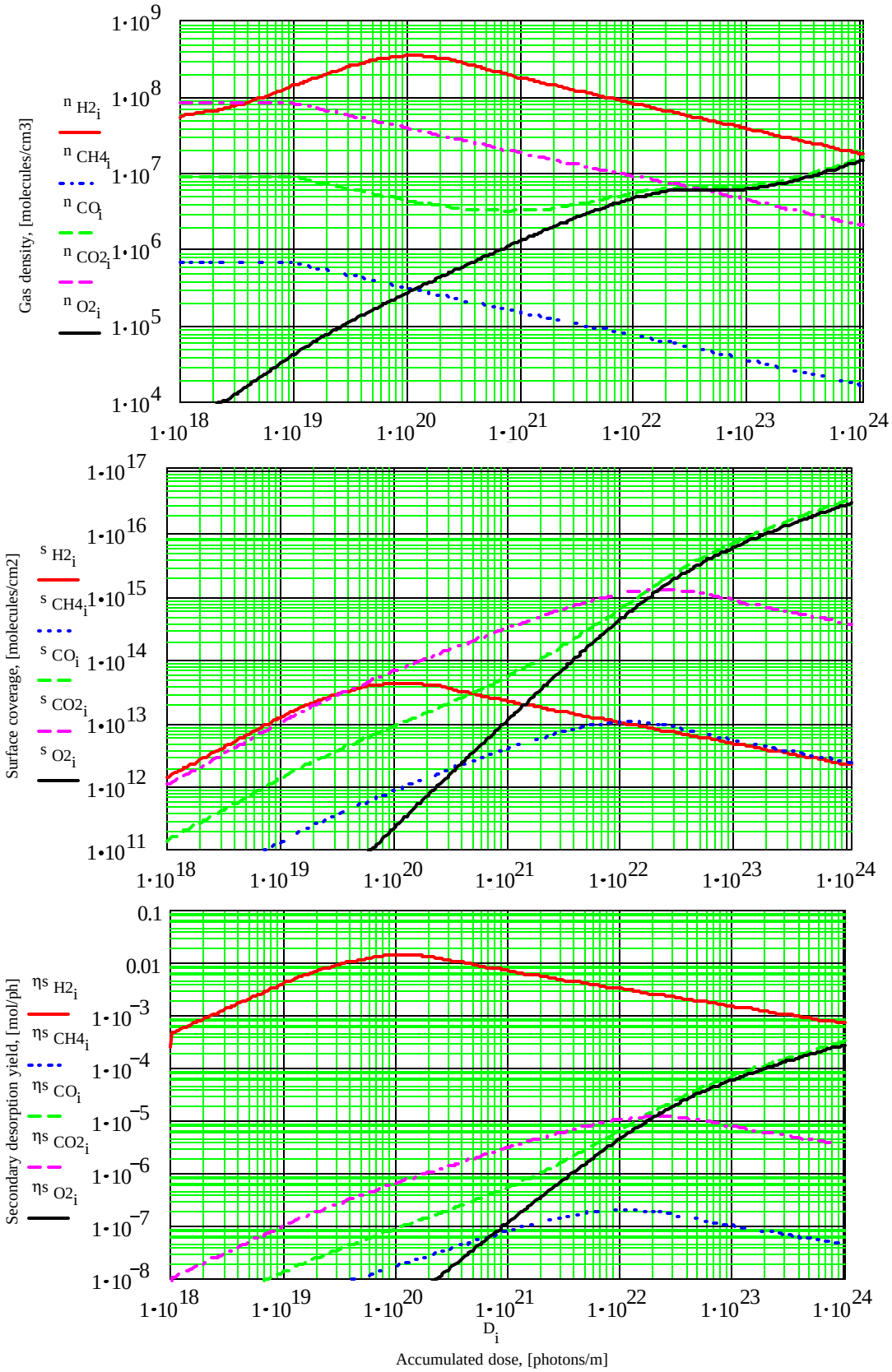

Figure 7. The gas density *n*, the surface coverage *s* and the photodesorption yield of cryosorbed molecules η' in a vacuum chamber with a beam screen at T=5K with $\eta(CO_2) >> \eta(CO)$, ($\alpha(H_2)=0.01$, $\alpha(CH_4,CO,CO_2)=1$).

As mentioned in Section 3.3 there exist an evidence that the sticking probability on a surface without precondensed gas could be much less than on the surface with condensed gas. The case with the sticking probability equal to zero all molecules of gas will be removed through the pumping holes, there is no gas condensed on the beam screen and, hence, no secondary desorption, and no transition in the gas density between the simple vacuum chamber estimation and the vacuum chamber with a beam screen as seen on Figures 2–7. The gas density depends only on the primary desorption yield of molecules and the distributed pumping speed of the beam screen slots:

$$n_i = \frac{h_i \dot{\Gamma}}{C_i} .$$

The estimation of gas density in the vacuum chamber with the beam screen for the zero sticking probability for all gases is shown in Figure 8. This case with the zero sticking probability is hardly improbable at the beam screen temperature of 5 K, however provides an upper limit of gas density for any sticking probability.

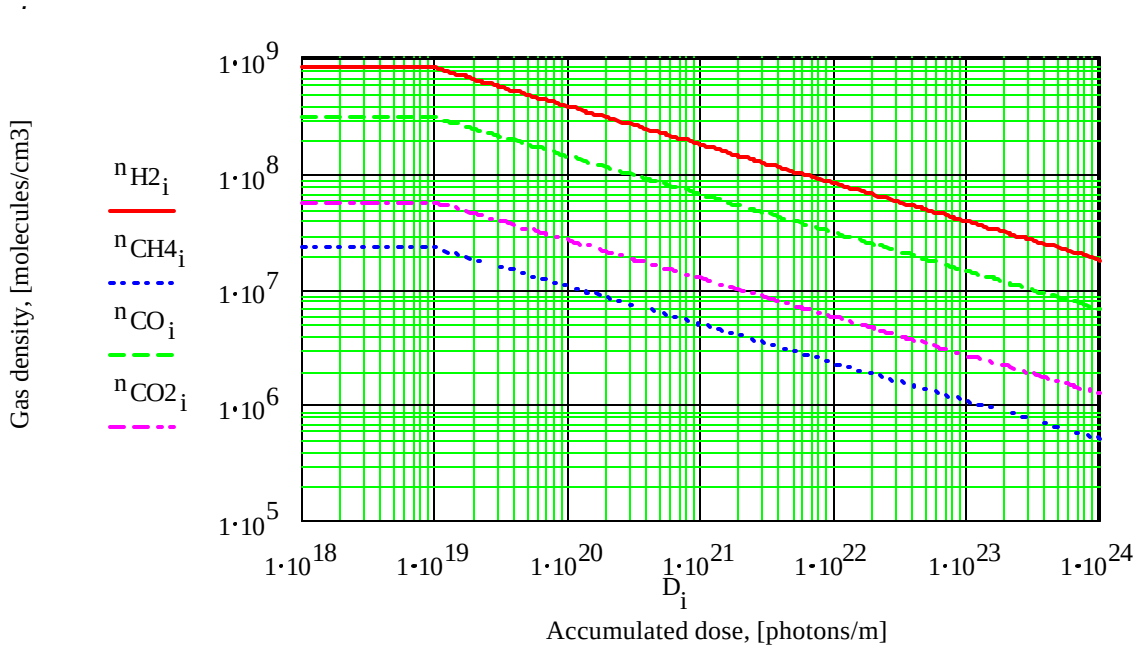

Figure 8. The upper limit of the gas density in a vacuum chamber with a beam screen at T=5K (a = 0).

6 Conclusions

- This study allows one to identify the dominant vacuum processes in a vacuum chamber with cryosorbing walls exposed to synchrotron radiation, to describe these processes using experimentally determined parameters and to estimate the gas density for various conditions.
- As an application to the LHC, it is shown that the dominating gases inside the LHC vacuum chamber with a beam screen are H_2 and CO.
- The amount of cryosorbed molecules of CH_4 and CO_2 is limited due to the cracking. The surface coverage of CO will increase continuously during the LHC lifetime without warm-up.
- This study also confirms that gas density inside that vacuum chamber with a beam screen will remain much below the beam lifetime limit also when taking into account the effect of cracking.
- When the LHC vacuum chamber will be warmed up after long time operation the main gases to be pumped out will be H_2, CO and perhaps O_2.

References:

1. V.V. Anashin, O.B. Malyshev, V.N. Osipov, I.L. Maslennikov and W.C. Turner. Investigation of Synchrotron Radiation-Induced Photodesorption in Cryosorbing Quasiclosed Geometry. J.Vac.Sci.Technol. A 12(5), pp. 2917–2921, Sep/Oct 1994.
2. V.V. Anashin, O.B. Malyshev, R. Calder, O. Gröbner and A.G. Mathewson. The study of photodesorption processes for cryosorbed CO_2. Nuclear Instruments & Methods in Physics Research A 405, 1998, pp. 258–261.
3. V.V. Anashin, O.B. Malyshev, R. Calder, O. Gröbner. A study of the photodesorption process for cryosorbed layers of H_2, CH_4, CO or CO_2 at varios temperatures between 3 and 68 K. Vacuum 53 (1999) 269–272.
4. V. Baglin. Etude de la photo-désorption de surfaces techniques aux températures cryogéniques. Doctorat thèse. Université Denis Diderot Paris & UFR de Physique, Paris, Mai 1997.

5. V.V. Anashin, G.E. Derevyankin, V.G. Dudnikov, O.B. Malyshev, V.N. Osipov, C.L. Foerster, F.M. Jacobsen, M.W. Ruckman, M. Strongin, R. Kersevan, I.L. Maslennikov, W.C. Turner and W.A. Landford. Cold Beam Tube Photodesorption and Related Experiments for SSCL 20 TeV Proton Collider. J.Vac.Sci.Technol. A 12(4), pp. 1663–1672, Jul/Aug 1994.

6. V. Anashin, O. Malyshev, V. Osipov, I. Maslennikov and W. Turner. Experimental Investigation of Dynamic Pressure in a Cryosorbing Beam Tube Exposed to Synchrotron Radiation. Proc. of EPAC-94, London, 27 June–1 July, 1994, v. 3, pp. 2506–2508.

7. N. Alinovsky, V. Anashin, P. Beschastny, G. Derevyankin, V. Dudikov, A. Evstigneev, A. Lysenko, O. Malyshev, V. Osipov, I. Maslennikov and W. Turner. A Hydrogen Ion Beam Method of Molecular Density Measurement Inside a 4.2K Beam Tube. Proc. of EPAC-94, London, 27 June–1 July, 1994, v. 3, pp. 2509–2511.

8. R. Calder, O. Gröbner, A.G. Mathewson, V.V. Anashin, A. Dranichnikov, O. Malyshev. Synchrotron radiation induced gas desorption from a prototype Large Hadron Collider beam screen at cryogenic temperatures. J.Vac.Sci.Technol. A 14(4), pp. 2618–2623, Jul/Aug 1996.

9. V.V. Anashin, O.B. Malyshev, R. Calder, O. Gröbner and A.G. Mathewson. Photon induced molecular desorption from condensed gases. Vacuum v. 48, No. 7–9, 1997, pp. 785–788.

10. V.V. Anashin, O.B. Malyshev, R. Calder, O. Gröbner. A study of the photodesorption process for cryosorbed layers H_2, CH_4, CO and CO_2 cryosorbed between 3 K and 68 K. Presented at IVC-98

11. V. Baglin. Measurement of the primary desorption yield at 4.2 K, 77 K and room temperature in a quasi-closed geometry. LHC Project Report 9. CERN, Geneva, 7 June 1997.

12. V.V. Anashin, G.E. Derevyankin, V.G. Dudnikov, O.B. Malyshev, V.N. Osipov, C.L. Foerster, F.M. Jacobsen, M.W. Ruckman, M. Strongin, R. Kersevan, I.L. Maslennikov, W.C. Turner and W.A. Landford. Cold beam tube photodesorption and related experiments for SSCL 20 TeV proton collider. J. Vac. Sci. Technol. A 12(4), pp. 1663–1672, Jul/Aug 1994.

13. W. Turner. Beam tube vacuum in future superconducting proton colliders. SSCL-Preprint-564. October 1994.

14. E. Wallén. Adsorption isotherms of H_2, CH_4, CO and CO_2 on a copper plated stainless steel at 4.2 K. J. Vac. Sci. Tech. A 14(5), Sep/Oct 1996, p. 2916.

15. O.B. Malyshev. A study of photodesorption process in vacuum chamber prototype of superconducting super collider. Thesis. 1995.

16. Y. Saito. Private discussion and information

17. C. Benvenuti, R.S. Calder and G. Passardi. Influence of thermal radiation on the vapor pressure of condensed hydrogen (and isotopes) between 2 and 4.5 K. J.Vac.Sci.Technol. V. 13, No. 6, Nov./Dec. 1996, pp.1172–1182

18. P.D. Bentley and B.A. Hands. The condensation of atmospheric gases on cold surface. Proc. R. Soc. Lond. A. 359, 319–343 (1978).